Steric Course and Mechanism of the Water Exchange of the Ruthenium(III) Aqua Pentaammine Ion

François P. Rotzinger[†]

Institut de Chimie Physique, Ecole Polytechnique Fédérale, CH-1015 Lausanne, Switzerland

Received: June 30, 1999; In Final Form: September 20, 1999

The water exchange on the ruthenium(III) aqua pentaammine ion was investigated using quantum chemical techniques. Calculations were performed for the free and the hydrated ions, with and without electron correlation (dispersion was neglected). The most accurate result was obtained when both hydration and correlation were considered. Two interchange pathways were investigated, one proceeding with retention of the configuration and the other one giving rise to stereomobility. The latter is unlikely to operate, because of its high activation energy. The computed energy of activation for the exchange with retention of the configuration (88 kJ/mol) is close to the measured $\Delta H_{298}^{\ddagger}/\Delta G_{298}^{\ddagger}$ values (91.5 and 93.8 kJ/mol, respectively). The dissociative mechanism does not operate because of its higher activation energy (103 kJ/mol).

Introduction

Among the aqua pentaammine complexes of inert trivalent transition metal ions, water exchange is fastest[1] at the ruthenium(III) center ($\Delta H_{298}^{\ddagger}/\Delta G_{298}^{\ddagger}$ = 91.5/93.8 kJ/mol). The moderately negative volume of activation[1] ($\Delta V^{\ddagger}$) of −4.0 cm^3/mol suggests the I_a mechanism for reaction 1. The strategy described

$$Ru(NH_3)_5OH_2^{3+} + \mathbf{H_2O} \rightarrow Ru(NH_3)_5\mathbf{OH_2}^{3+} + H_2O \quad (1)$$

in previous work[2−4] on the water exchange of metal hexaaqua ions, where the interchange mechanisms were investigated on the basis of the activation of the water adducts of the reactants (eq 2) was also applied to the present system. Although the

$$Ru(NH_3)_5OH_2\cdot OH_2^{3+} \rightarrow [Ru(NH_3)_5\cdots(OH_2)_2^{3+}]^{\ddagger} \quad (2)$$

steric course of reaction 1 is not yet known experimentally, two transition states have been calculated for the interchange pathway: one giving rise to retention of the configuration (reaction 3a) and the other one to stereomobility, where, for example, a trans $^{15}NH_3$ ligand would end in the cis position after the exchange of the water ligand (reaction 3b). The

$$trans\text{-}Ru(NH_3)_4(^{15}NH_3)OH_2^{3+} + \mathbf{H_2O} \rightarrow trans\text{-}Ru(NH_3)_4(^{15}NH_3)\mathbf{OH_2}^{3+} + H_2O \quad (3a)$$

$$trans\text{-}Ru(NH_3)_4(^{15}NH_3)OH_2^{3+} + \mathbf{H_2O} \rightarrow cis\text{-}Ru(NH_3)_4(^{15}NH_3)\mathbf{OH_2}^{3+} + H_2O \quad (3b)$$

dissociative (D) mechanism is always feasible[2,3] and was investigated on the basis of eq 4. Since for the low-spin d^5 electron configuration, no trigonal bipyramidal transition state

$$Ru(NH_3)_5OH_2^{3+} \rightarrow [Ru(NH_3)_5\cdots OH_2^{3+}]^{\ddagger} \quad (4)$$

is formed,[3] this mechanism would proceed with retention of the configuration. For all above-mentioned mechanisms, the quantum chemical computations were performed for the free ions, similar to the computations[2−4] on the metal hexaaqua ions, and the hydrated ions. Furthermore, electron correlation in the complexes was taken into account, but not the dispersion (correlation of solute and solvent). The two models, treating the free and solvated ions and the two computational levels with or without electron correlation are compared.

Results

All geometries (Table 1) have been optimized for the free and the hydrated ions at the Hartree−Fock level. For the latter, the calculations were performed using the self-consistent reaction field (SCRF) model.[5−7] The energy of the free ions (Table 2) was computed at the Hartree−Fock (HF) and "multiconfigurational self-consistent field second-order quasidegenerate perturbation" (MCQDPT2) level,[8,9] which takes into account static and dynamic electron correlation. The energy of the hydrated ions (Table 2) was computed on the basis of the polarizable continuum model (PCM)[10−12] at the HF or CAS-SCF level, and the contribution due to dynamic correlation was obtained as a second-order perturbation of the CAS-SCF wave function (see Computational Details). The latter technique is the most accurate, but also most the demanding, one. The activation energies were computed by neglecting the zero point energy. Therefore, the $\Delta E^{\ddagger}$ values correspond approximately to the Eyring enthalpy of activation $\Delta H^{\ddagger}$. The activation energies for reactions 3a, 3b, and 4, based on the above-described models and techniques, are summarized in Table 3.

Other approximations, the model, and its limitations were discussed previously.[2−4] Therefore, these arguments are not repeated here.

Water Exchange with Retention of the Configuration. In aqua pentaammine complexes, the two halves of the octahedron are inequivalent. The attack of a nucleophile on its "upper half", defined here by the water and the four equatorial ammonia ligands, gives rise to a product where the configuration of the ammonia ligands is retained. Water exchange according to this mechanism (reaction 3a), where the nucleophile enters adjacent

[†] Tel: ++41 21 693 36 09. Fax: ++41 21 693 41 11. E-mail: francois.rotzinger@epfl.ch.

10.1021/jp992249c CCC: $18.00
Published on Web 10/30/1999

TABLE 1: Ruthenium−Ligand Bond Lengths and Changes of Their Sum during the Activation

species	d(Ru−N), Å	d(Ru−O), Å	$\sum d$(Ru−L), Å	$\Delta\sum d$(Ru−L), Å
	(i) Geometries of the Free Ions			
$Ru(NH_3)_5OH_2{\cdot}OH_2^{3+}$	2.219, 2.197, 2.185, 2.200, 2.197	2.118, 4.019	17.135	0.0
$[cis\text{-}Ru(NH_3)_5\cdots(OH_2)_2^{3+}]^{\ddagger}$	2.199, 2.203, 2.157, 2.207, 2.205	2.684, 2.636	16.291	−0.844
$[Ru(NH_3)_5\cdots(OH_2)_2^{3+}]^{\ddagger}$	2.274, 2.213, 2.198, 2.131[a]	2.867[a]	16.681	−0.454
$Ru(NH_3)_5OH_2^{3+}$	2.192, 2.200, 2.186, 2.199, 2.190	2.212	12.179	0.0
$[Ru(NH_3)_5\cdots OH_2^{3+}]^{\ddagger}$	2.171[a], 2.132, 2.200[a]	3.462	14.336	2.157
	(ii) Geometries of the Hydrated Ions			
$Ru(NH_3)_5OH_2{\cdot}OH_2^{3+}$	2.216, 2.198, 2.182, 2.199, 2.200	2.124, 4.048	17.167	0.0
$[cis\text{-}Ru(NH_3)_5\cdots(OH_2)_2^{3+}]^{\ddagger}$	2.198, 2.202, 2.152, 2.205, 2.204	2.717, 2.670	16.348	−0.819
$[Ru(NH_3)_5\cdots(OH_2)_2^{3+}]^{\ddagger}$	2.278, 2.212, 2.199, 2.130[a]	2.866[a]	16.681	−0.486
$Ru(NH_3)_5OH_2^{3+}$	2.192, 2.200, 2.185, 2.199, 2.191	2.214	12.181	0.0
$[Ru(NH_3)_5\cdots OH_2^{3+}]^{\ddagger}$	2.176[a], 2.130, 2.196[a]	3.446	14.320	2.139

[a] Two symmetry equivalent bonds.

TABLE 2: Total Energies[a] of All Computed Species

	free ion		hydrated ion	
species	HF	MCQDPT2[b]	PCM(HF)	PCM(CAS-SCF) + MP2[b]
$Ru(NH_3)_5OH_2{\cdot}OH_2^{3+}$	−525.345096	−526.710249 (8)	−525.950190	−527.314580 (8)
$[cis\text{-}Ru(NH_3)_5\cdots(OH_2)_2^{3+}]^{\ddagger}$	−525.304543	−526.669269 (8)	−525.916466	−527.281119 (8)
$[Ru(NH_3)_5\cdots(OH_2)_2^{3+}]^{\ddagger}$	−525.290579	−526.664142 (4)	−525.896360	−527.268465 (75)
$Ru(NH_3)_5OH_2^{3+}$	−449.276904	−450.449900 (210)	−449.912928	−451.083175 (210)
$[Ru(NH_3)_5\cdots OH_2^{3+}]^{\ddagger}$	−449.244544	−450.418236 (108)	−449.870599	−451.044037 (210)

[a] Units: hartrees. [b] In parentheses: number of configuration state functions.

TABLE 3: Activation Energies[a] for Pathways 3a, 3b, and 4

	free ion		hydrated ion[b]	
species	HF	MCQDPT2	PCM(HF)	PCM(CAS-SCF) + MP2
$[cis\text{-}Ru(NH_3)_5\cdots(OH_2)_2^{3+}]^{\ddagger}$	106.5	107.6	88.5	87.9
$[Ru(NH_3)_5\cdots(OH_2)_2^{3+}]^{\ddagger}$	143.1	121.1	141.3	121.1
$[Ru(NH_3)_5\cdots OH_2^{3+}]^{\ddagger}$	85.0	83.1	111.1	102.8

[a] Units: kJ/mol. [b] Experimental values: $\Delta H^{\ddagger}_{298} = 91.5$ and $\Delta G^{\ddagger}_{298} = 93.8$ kJ/mol.[1]

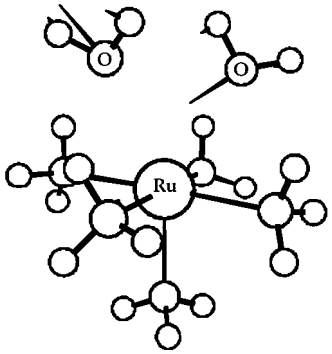

Figure 1. Perspective view and imaginary mode of the transition state $[cis\text{-}Ru(NH_3)_5\cdots(OH_2)_2^{3+}]^{\ddagger}$ (interchange mechanism, attack adjacent to the leaving ligand).

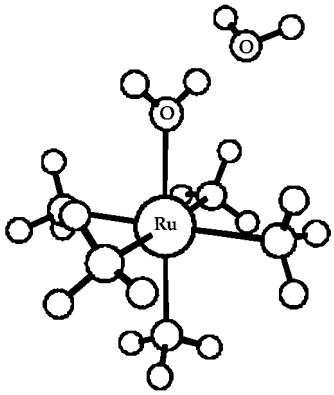

Figure 2. Perspective view of the reactant or product $Ru(NH_3)_5OH_2{\cdot}OH_2^{3+}$.

to the leaving H_2O ligand, involves the transition state $[cis\text{-}Ru(NH_3)_5\cdots(OH_2)_2^{3+}]^{\ddagger}$ (Figure 1), which was obtained by previously described techniques.[2,3,13] The imaginary mode, which is the reaction coordinate, shows that this exchange is a concerted process. The relatively short Ru···O bonds in the transition state, which has no symmetry (Table 1), are typical of the I_a mechanism. The reactant or product (Figure 2) was obtained by the computation of the intrinsic reaction coordinate, along which no intermediate was found. Since the transition state $[cis\text{-}Ru(NH_3)_5\cdots(OH_2)_2^{3+}]^{\ddagger}$ has no symmetry, the intrinsic reaction coordinates leading to the reactant or product are different. For the analogous water exchange via $[cis\text{-}Rh(NH_3)_5\cdots(OH_2)_2^{3+}]^{\ddagger}$, the reactant as well as the product were identical despite the different reaction coordinates.[13] Hence, for the very similar transition state $[cis\text{-}Ru(NH_3)_5\cdots(OH_2)_2^{3+}]^{\ddagger}$, reactant and product are expected to have the same structures, too. Therefore, only one intrinsic reaction coordinate was computed. The entering or exchanged water molecule, located in the "upper half" of the octahedron, is hydrogen bonded to the aqua and one ammonia ligand. The change of the sum of the Ru−L bond lengths, $\Delta\sum d$(Ru−L), is negative (Table 1) indicating again that (3a) involves an **a** activation. The inclusion of hydration leads to small bond length changes (<0.04 Å), and more importantly, the mechanistically diagnostic $\Delta\sum d$(Ru−L) parameter changed very slightly. Whether the geometry of the free ion or that of the hydrated one is taken, or whether electron correlation is included, the computed energy of activation differs from the experimental[1] $\Delta H^{\ddagger}$ or $\Delta G^{\ddagger}$ value of 91.5 or 93.8 kJ/mol, respectively, by less than 15 kJ/mol. As expected, the computed

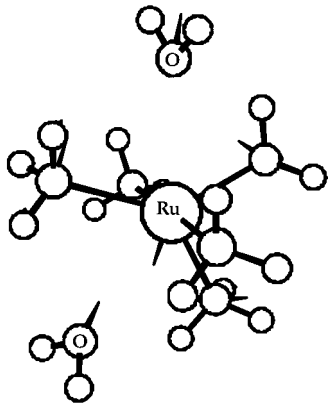

Figure 3. Perspective view and imaginary mode of the transition state $[Ru(NH_3)_5\cdots(OH_2)_2^{3+}]^{\ddagger}$ with C_s symmetry (interchange mechanism, attack opposite to the leaving ligand).

values based on the hydrated ions are closest to the observed ones.

Water Exchange with Stereomobility. In contrast to the previous case, the attack of a nucleophile on the "lower half" of the octahedron, defined by the five ammonia ligands, leads to stereomobility, where the ammonia ligand having been originally in the apical position ends up in the equatorial plane (reaction 3b). The corresponding transition state $[Ru(NH_3)_5\cdots(OH_2)_2^{3+}]^{\ddagger}$, resulting from the attack opposite to the leaving group, is a pentagonal bipyramid having C_s symmetry (Figure 3). The imaginary mode describes the concerted entry and leaving of the exchanging water molecules together with the rearrangement of the three ammonia ligands in the trigonal RuN_3 plane. The corresponding reactant or product was not computed; it would resemble that of (3a) (Figure 2) with the water molecule of the second coordination sphere being located in the "lower half" of the octahedron and hydrogen bonded to ammonia ligands only. For this transition state, the (symmetry equivalent) Ru···O bonds are longer by about 0.2 Å than those of the corresponding cis isomer, and therefore, the $\Delta\sum d$(Ru−L) value for this pathway (reaction 3b) is less negative (Table 1). This suggests that also this exchange would proceed via the I_a mechanism, but with a less negative volume of activation than (3a). Whether electron correlation is included or not, the computed activation energies are insensitive to hydration. Unlike the activation energy for (3a) that is sensitive to hydration, but not to correlation, the inclusion of the latter lowers the activation energy by 20 kJ/mol. Since this pathway (reaction 3b) requires a significantly higher activation energy (33.2 kJ/mol) than (3a), the interchange mechanism is expected to proceed quantitatively with retention of the configuration.

Dissociative Mechanism. The activation energy for this always feasible, but not always most favorable pathway,[2,3] was calculated on the basis of eq 4. The transition state $[Ru(NH_3)_5\cdot\cdot\cdot OH_2^{3+}]^{\ddagger}$, which has C_s symmetry, together with its imaginary mode are shown in Figure 4. As expected for a dissociative activation, the Ru···O bond is much longer than in the transition state for each of the interchange mechanisms, and the change in the sum of the Ru−L bond lengths during the activation, $\Delta\sum d$(Ru−L), is large and positive (Table 1). The activation energy for this pathway, calculated using the best method that takes into account hydration and electron correlation (Table 3), lies between the activation energies of the two interchange mechanisms. The D mechanism is less favorable by 15 kJ/mol than the interchange mechanism, which involves retention of the configuration, but is more advantageous than the interchange pathway involving stereomobility. The D mechanism would

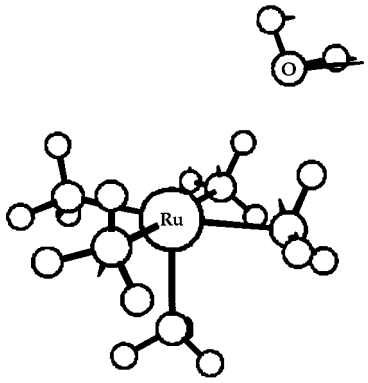

Figure 4. Perspective view and imaginary mode of the transition state $[Ru(NH_3)_5\cdots OH_2^{3+}]^{\ddagger}$ (D mechanism).

proceed with retention of the configuration, since for a low-spin d^5 electron configuration the trigonal bipyramidal pentacoordinated intermediate is less stable than the square pyramidal one.[3] A detailed analysis of this mechanism will be given for the water exchange on $Rh(NH_2CH_3)_5OH_2^{3+}$ and $Rh(NH_3)_5OH_2^{3+}$.[13]

It is interesting to note that according to the calculations on the free ions in the gas phase, the D mechanism is more favorable than the interchange one by 25 kJ/mol (Table 3). The relative ordering of the activation energies does not depend on the geometries, since the inclusion of hydration leads to very small geometry changes (Table 1). It is the hydration energy of the two transition states for the interchange and that for the dissociative mechanism that are different. The inclusion of hydration lowers the activation energy by 20 kJ/mol for (3a), has no effect on that of (3b), and increases that for (4) by 20 kJ/mol.

Discussion

Role of the Computational Model. When hydration is included, the activation energy for reaction 3a, which is reaction 1 proceeding with retention of the configuration, agrees with the experimental[1] $\Delta H_{298}^{\ddagger}/\Delta G_{298}^{\ddagger}$ values, although specific effects of hydrogen bonding with the bulk solvent were not considered (neither in the geometry optimizations nor in the energy computations). This omission leads to systematic errors, leading to Ru−L bond lengths that are too long. Also the geometry optimization at the Hartree−Fock level gives rise to longer Ru−L bond lengths, as discussed previously.[2,3] Therefore, all the computed geometries suffer from too long Ru−L bonds. The energies, on the other hand, appear more accurate.

The activation energies for reactions 3a and 4 are sensitive to *hydration*, but that of 3b is sensitive to *correlation*. Furthermore, depending on the kind of reaction, hydration can lower or raise the activation energy as seen for (3a) and (4), respectively. This observation suggests that the effects of hydration and correlation cannot be predicted a priori. Although the corresponding corrections are not large ($\leq$26 kJ/mol in the present cases), they are unavoidable, if the most favorable pathway has to be determined.

Stereochemistry of the Water Exchange. Reaction 1 is unlikely to proceed with stereomobility, since reaction 3b is predicted to contribute less than 1% regardless of the applied model and computational method. This result should, however, not be generalized for amine complexes of ruthenium(III) with bulky or chelating ligands, since strain or constraints in the ligand sphere could alter the activation energies for (3a) and (3b) considerably by favoring or disfavoring one of the two

pathways. It is important to note that the D mechanism requires an activation energy that is higher by only 15 kJ/mol than the most favorable interchange one (Table 3). For the present system, $Ru(NH_3)_5OH_2^{3+}$, it does not operate, as already postulated on the basis of the experimental[1] negative volume of activation. In complexes with bulky or chelating amine ligands, however, the D pathway might become competitive or even favorable, as in $Rh(NH_2CH_3)_5OH_2^{3+}$.[13]

Electronic Structure of the Transition States. The stability of heptacoordinated species depends on the spin state and the number of d electrons. This has been shown[3] for the water exchange on the first row transition metal hexaaqua ions. According to these criteria, the two present transition states, $[cis\text{-}Ru(NH_3)_5\cdots(OH_2)_2^{3+}]^{\ddagger}$ and $[Ru(NH_3)_5\cdots(OH_2)_2^{3+}]^{\ddagger}$, which have a low-spin d^5 electron configuration, are predicted to be accessible, since 4 electrons are located in nonbonding orbitals (d_α levels in ref 3) and a single electron is in a slightly antibonding (d_β) level.

Computational Details

All the calculations have been performed on Cray T3D, HP 9000/C200, and HP 9000/735 computers using the GAMESS[14] programs.

The basis sets of Stevens, Basch, Krauss, and Jasien[15] were used for ruthenium, where the 1s, 2s, 3s, 2p, 3p, and 3d shells are represented by relativistic effective core potentials, the 4s, 4p, 5s, and 5p shells have double-ζ quality, and the 4d has triple-ζ quality. For N, O, and H, 6-31G(d) basis sets[16,17] were used ($\alpha_{3d} = 1.00$ and 1.20,[18] respectively).

For the SCRF calculations,[5−7] the cavity radius was taken as half of the value of the largest interatomic distance plus the two corresponding van der Waals radii. Once the geometry had converged, the cavity radius was redetermined, and if it differed by more than 0.01 Å form the previous value, the geometry optimization was repeated until the above criterion was fulfilled. All atomic coordinates (for the free and the hydrated ions) are summarized in Tables S1−S5.

The active space for the CAS-SCF and multiconfigurational self-consistent field second-order quasidegenerate perturbation (MCQDPT2)[8,9] calculations was determined using the iterative natural orbital (INO) method.[19] Natural orbitals of a final CAS-CI calculation with occupations ≥ 0.015 were used for the active space of the CAS-SCF or MCQDPT2 steps. The energy computations based on the polarizable continuum model (PCM)[10−12] were performed at the CAS-SCF level, and the second-order perturbation energy of this wave function was calculated using the MCQDPT2 code (at the in vacuo level); the second-order contribution is equal to the second-order minus the first-order energy, $E(\mathrm{MP2}) - E(\mathrm{MCSCF})$. The total PCM energy, corrected by second-order perturbation, is equal to the PCM energy (CAS-SCF level) plus the above second-order correction.

The zero point energy was neglected for the reasons discussed in previous work.[2,3]

Acknowledgment. Prof. Dr. E. Sánchez Marcos is acknowledged for a valuable hint, and Dr. R. Humphry-Baker, for helpful comments to the manuscript.

Supporting Information Available: A listing of the atomic coordinates of the reactants/products and the transition states for the activation according to eqs 3a, 3b, and 4 (Tables S1−S5). This information is available free of charge via the Internet at http://pubs.acs.org.

References and Notes

(1) Doine, H.; Ishihara, K.; Krouse, H. R.; Swaddle, T. W. *Inorg. Chem.* **1987**, *26*, 3240.
(2) Rotzinger, F. P. *J. Am. Chem. Soc.* **1996**, *118*, 6760.
(3) Rotzinger, F. P. *J. Am. Chem. Soc.* **1997**, *119*, 5230.
(4) Kowall, Th.; Caravan, P.; Bourgeois, H.; Helm, L.; Rotzinger, F. P.; Merbach, A. E. *J. Am. Chem. Soc.* **1998**, *120*, 6569.
(5) Kirkwood, J. G. *J. Chem. Phys.* **1934**, *2*, 351.
(6) Onsager, L. *J. Am. Chem. Soc.* **1936**, *58*, 1486.
(7) Szafran, M.; Karelson, M. M.; Katritzky, A. R.; Koput, J.; Zerner, M. C. *J. Comput. Chem.* **1993**, *14*, 371.
(8) Nakano, H. *J. Chem. Phys.* **1993**, *99*, 7983.
(9) Nakano, H. *Chem. Phys. Lett.* **1993**, *207*, 372.
(10) Miertus, S.; Scrocco, E.; Tomasi, J. *Chem. Phys.* **1981**, *55*, 117.
(11) Tomasi, J.; Persico, M. *Chem. Rev.* **1994**, *94*, 2027.
(12) Tomasi, J.; Cammi, R. *J. Comput. Chem.* **1995**, *16*, 1449.
(13) Rotzinger, F. P. Work in progress.
(14) Schmidt, M. W.; Baldridge, K. K.; Boatz, J. A.; Elbert, S. T.; Gordon, M. S.; Jensen, J. H.; Koseki, S.; Matsunaga, N.; Nguyen, K. A.; Su, S. J.; Windus, T. L.; Dupuis, M.; Montgomery, J. A. *J. Comput. Chem.* **1993**, *14*, 1347.
(15) Stevens, W. J.; Krauss, M.; Basch, H.; Jasien, P. G. *Can. J. Chem.* **1992**, *70*, 612.
(16) Hehre, W. J.; Ditchfield, R.; Pople, J. A. *J. Chem. Phys.* **1972**, *56*, 2257.
(17) Ditchfield, R.; Hehre, W. J.; Pople, J. A. *J. Chem. Phys.* **1971**, *54*, 724.
(18) Schäfer, A.; Horn, H.; Ahlrichs, R. *J. Chem. Phys.* **1992**, *97*, 2571.
(19) Bender, C. F.; Davidson, E. R. *J. Phys. Chem.* **1966**, *70*, 2675.